Inorganic Chemistry
Article

Inorg. Chem. **2011**, *50*, 1203–1212 **1203**
DOI: 10.1021/ic101460z

Real-Time High-Resolution X-ray Imaging and Nuclear Magnetic Resonance Study of the Hydration of Pure and Na-Doped C_3A in the Presence of Sulfates

A. P. Kirchheim,*,†,⊥ D. C. Dal Molin,† P. Fischer,‡ Abdul-Hamid Emwas,§ J. L. Provis,∥ and P. J. M. Monteiro⊥

†*Department of Civil Engineering, Federal University of Rio Grande do Sul, Porto Alegre, RS, Brazil,* ‡*Center for X-ray Optics, Lawrence Berkeley National Laboratory, Berkeley, California, United States,* §*NMR Core lab, King Abdullah University of Science and Technology, Thuwal 23955-6900, Kingdom of Saudi Arabia,* ∥*Department of Chemical & Biomolecular Engineering, University of Melbourne, Victoria 3010, Australia, and* ⊥*Department of Civil and Environmental Engineering, University of California, Berkeley, California, United States*

Received July 21, 2010

This study details the differences in real-time hydration between pure tricalcium aluminate (cubic C_3A or $3CaO \cdot Al_2O_3$) and Na-doped tricalcium aluminate (orthorhombic C_3A or $Na_2Ca_8Al_6O_{18}$), in aqueous solutions containing sulfate ions. Pure phases were synthesized in the laboratory to develop an independent benchmark for the reactions, meaning that their reactions during hydration in a simulated early age cement pore solution (saturated with respect to gypsum and lime) were able to be isolated. Because the rate of this reaction is extremely rapid, most microscopy methods are not adequate to study the early phases of the reactions in the early stages. Here, a high-resolution full-field soft X-ray imaging technique operating in the X-ray water window, combined with solution analysis by ^{27}Al nuclear magnetic resonance (NMR) spectroscopy, was used to capture information regarding the mechanism of C_3A hydration during the early stages. There are differences in the hydration mechanism between the two types of C_3A, which are also dependent on the concentration of sulfate ions in the solution. The reactions with cubic C_3A (pure) seem to be more influenced by higher concentrations of sulfate ions, forming smaller ettringite needles at a slower pace than the orthorhombic C_3A (Na-doped) sample. The rate of release of aluminate species into the solution phase is also accelerated by Na doping.

1. Introduction

The properties of cement clinkers are strongly affected by the quantity and composition of the clinker phases,[1] which can drive the kinetics of the process of hydration. In ordinary Portland cement, the average abundances of these phases vary between 50% and 70% of alite (tricalcium silicate, $3CaO \cdot SiO_2$; abbreviated by cement chemists as C_3S), between 15% and 30% of belite (dicalcium silicate, $2CaO \cdot SiO_2$; abbreviated C_2S), between 5% and 10% of tricalcium aluminate ($3CaO \cdot Al_2O_3$ or C_3A), and between 5% and 15% of tetracalcium aluminoferrite ($4CaO \cdot Al_2O_3 \cdot Fe_2O_3$ or C_4AF). However, the chemical compositions of compounds present in the industrial Portland cements do not exactly correspond to what is expressed by the commonly used abbreviated formulas (C_3S, C_2S, C_3A, and C_4AF). This is because at the high temperatures prevalent during clinker formation the impurity elements present in the system, including magnesium, sodium, potassium, and sulfur, enter into solid solutions with each of the major clinker compounds. Small amounts of impurities in a solid solution may not significantly alter the crystallographic nature of a compound or its reactivity with water, but larger amounts can do so. The alkalis, mainly sodium and potassium, in Portland cement clinker are derived mainly from the clay components present in the raw mix and coal; their total amount, expressed as Na_2O equivalent ($Na_2O + 0.64K_2O$), may range from 0.3 to 1.5%.[4]

The hydration of tricalcium aluminate (C_3A) is an important stage in the overall hydration of cement because it has a considerable influence on setting and early hardening. The hydration of C_3A is far more strongly affected by environmental conditions than that of C_3S and, in particular, by the presence of other substances with which it can react.[8] The reaction of C_3A with water is of course a primary consideration. Calcium aluminate hydrates (e.g., C_3AH_6, C_4AH_{19}, and C_2AH_8) form quickly and liberate large amounts of heat.[9] If the very rapid and exothermic hydration of C_3A is allowed to proceed unhindered in cement, setting occurs too quickly and

*To whom correspondence should be addressed. Phone: +55 51 3308 4439. Fax: +55 51 3308 3321. E-mail: anapaula.k@gmail.com.

(1) Goetz-Neunhoeffer, F.; Neubauer, J. Crystal structure refinement of Na-substituted C_3A by Rietveld analysis and quantification in OPC. *Proceedings 10th International Congress on the Chemistry of Cement*, Göteborg, Sweden, 1997; Vol *1*.

Published on Web 01/19/2011

the cement paste does not develop strength. Therefore, calcium sulfate (as gypsum and/or anhydrite) is added to slow down the C_3A hydration. In the presence of calcium sulfate, C_3A forms needle-like ettringite. Thus, for practical purposes, it is not the hydration reaction of C_3A alone that is important, but rather the hydration reaction of C_3A in the presence of gypsum (i.e., soluble sulfates). The reactivity of C_3A in clinker and the availability of sulfate in solution control the setting characteristics of concrete, making the understanding of these compounds essential in addressing potential setting problems.

Because of the high content of C_3A in some cements, special attention must be paid to the mineralogy and reactivity of this phase. Industrial clinkers and their phases contain minor components such as Na_2O, K_2O, SO_3, and Cl^-, which may be attributed to several sources, including raw materials, fuel, and/or the lining of the kilns. Alkalis can be incorporated into a number of phases of the clinker, and often Na_2O is taken up by the C_3A.[2] When C_3A is synthesized in the presence of alkalis, its crystal lattice changes and the formation of the other phases occur.[3] There are several series of solid solutions with the general formula $Na_{2x}Ca_{3-x}Al_2O_6$, including a cubic C_3A with $0 < x < 0.10$, an orthorhombic C_3A with $0.16 < x < 0.20$, and a monoclinic C_3A with $0.20 < x < 0.25$.[4,5]

In Portland cements, cubic and orthorhombic C_3A are found alone or in combination; the monoclinic modification is not observed. The cubic phase is often finely grained and closely mixed with dendritic crystals of ferrite (C_4AF, tetracalcium aluminoferrite). The orthorhombic modification occurs as a prismatic, dark interstitial material, and is sometimes pseudo-tetragonal.[4] In the orthorhombic structure, the replacement of Na^+ at a calcium site can only occur at the Ca_5 site, which causes the polyhedron to expand.[6] In industrial clinkers, a more typical mechanism of formation of this phase is the metastable extension of the solid solution series accompanied by rapid cooling.[5] In cement, higher percentages of Na_2O in the raw materials lead to formation of orthorhombic C_3A.[7]

This paper aims to clarify the early hydration mechanism of cubic and orthorhombic C_3A using advanced in situ techniques, specifically soft X-ray microscopy, which allows the study of hydration in a wet environment with submicrometer spatial resolution. The present study uses pure components of cubic C_3A (pure) and orthorhombic C_3A (Na-doped), synthesized in a laboratory. This allows isolation and observation of the effects of each crystalline form of the aluminate in a given environment, which would not be possible if cement particles (containing several different phases) were used. Analysis of the supernatant solution by ^{27}Al NMR spectroscopy provides additional information regarding the structure and role of the aluminate species released into the sulfate-containing solution. Different concentrations of sulfate ions are analyzed to understand how each aluminate phase reacts under different conditions. This study is part of a larger program of work[10,11] which includes the study of these materials in other conditions and using other techniques.

Table 1. Particle Size Distribution of the Samples from Laser Granulometry

	cubic C_3A (μm)	orthorhombic C_3A (μm)
10th percentile diameter	5.74	1.64
50th percentile diameter	24.31	16.04
90th percentile diameter	45.00	36.34
mean diameter	25.16	18.43

2. Experimental Section

2.1. Materials. Samples of tricalcium aluminate (C_3A), both orthorhombic (Na-doped) and cubic (pure), were obtained from Construction Technology Laboratories, Inc., Skokie, IL. Both compounds were synthesized in a laboratory by heating a stoichiometric blend of reagent grade $CaCO_3$ and alumina (Al_2O_3) in an electric furnace at 1400 °C for 1 h, followed by quenching in air. The orthorhombic C_3A was prepared from reagent grade $CaCO_3$, Al_2O_3, and Na_2CO_3 in stoichiometric proportions, similar to the process reported by Regourd et al.,[12] with the latter slightly added in excess to account for alkali volatilization during the synthesis process. After synthesis, each material was processed in a ceramic mill to pass 325 mesh.

X-ray diffraction (XRD, PANalytical XPert Pro) and thermogravimetric analysis (TGA, TA Instruments, SDT 2960, 10 °C/min, N_2 gas, 100 mL/min) were conducted to confirm the phase composition, purity, and condition of the samples. Comparisons of the XRD peak positions were made with data from Regourd et al.[12] (ICDD PDF No.38-1429 for the cubic sample and ICDD PDF No.26-0958 for the orthorhombic). The TGA data showed that the samples were not hydrated by the ambient moisture, because both samples presented a low loss of mass upon heating, less than 1% and 8%, respectively, for the cubic and orthorhombic samples.

Particle size distributions of the samples were measured in a CILAS 1180 Laser Granulometer, in liquid isopropyl alcohol of 99.5% purity; the results are presented in Table 1. The lower size limit of this equipment was 40 nm, and the Fraunhofer approximation was applied in analysis of the data.

2.2. Sample Preparation. 2.2.1. Imaging with Soft X-ray Microscopy. Soft X-ray microscopy operating in the water window, that is, at a photon wavelength of about 2.4 nm, combines high spatial resolution in the tens of nanometers range with the ability to penetrate several micrometers of aqueous solution, making it an ideal in situ technique to study wet and nanostructured materials. The high spatial resolution of this microscopy technique is well suited to observing the formation of ettringite crystals around calcium aluminate grains and in solution, and to see the differences between the hydrates formed from cubic and orthorhombic C_3A. Furthermore, because the sample is kept wet at all times, it is possible to observe the progression of hydration over time.

Real-time hydration studies with soft X-ray transmission microscopy were carried out at the full field soft X-ray microscopy end-station XM-1 located at beamline 6.1.2 at the

(2) Spierings G.ACM, Stein H. N. *Cem. Concr. Res.*, **1976**. *6*(2): p. 265-272.
(3) Wachtler, H.-J. *Silikattechnick* **1986**, *4*, 127–131.
(4) Taylor, H. F. W. *Cement Chemistry*; Academic Press: London, 1990.
(5) Maki, I. *Cem. Concr. Res.* **1973**, *3*(3), 295–313.
(6) Takeuchi, Y.; Nishi, F.; et al. Structural aspect of the C_3A-Na_2O solid solutions. *Proceedings 7th International Congress on the Chemistry of Cement*, Paris, 1980; pp 426−431.
(7) Gobbo, L.; Sant'agostino, L.; et al. *Cem. Concr. Res.* **2004**, *34*(4), 657–664.
(8) Massazza, F.; Daimon, M. Chemistry of Hydration of Cements and Cementitious systems. *Proceedings 9th International Congress on the Chemistry of Cement*, New Delhi, India, 1992.
(9) Mehta, P. K.; Monteiro, P. J. M. *Concrete - Microstructure, Properties and Materials*, 3rd ed.; McGraw-Hill: New York. 2006.
(10) Kirchheim A. P. Cubic and orthorhombic tricalcium aluminate: analysis of in situ hydration and products. Ph.D. Thesis (in Portuguese), Federal University of Rio Grande do Sul, Porto Alegre, Brazil, 2008.
(11) Kirchheim, A. P. *J. Mater. Sci.* **2009**, No. 44, 2038–2045.
(12) Regourd, M.; Chromy, S.; Hjoth, L.; Mortureux, B.; Guinier, A. *J. Appl. Crystallogr.* **1973**, *6*, 355–364.

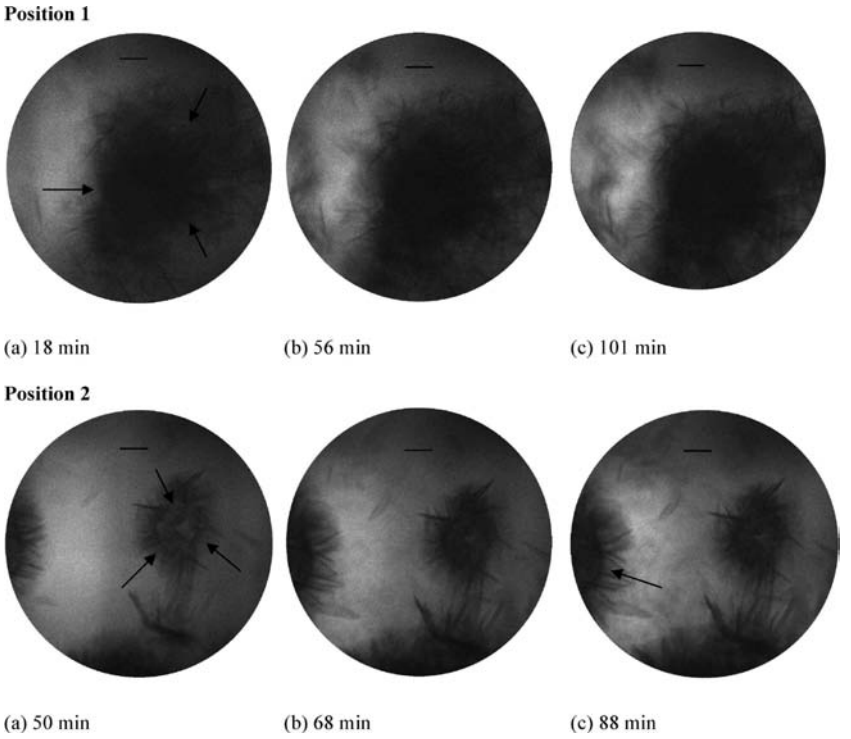

Figure 1. In situ soft X-ray images of hydrating cubic C_3A particles in a saturated calcium hydroxide-gypsum solution, $s/a_{initial} = 5$ mL/g. Hydration time is indicated. Scale bars correspond to 1 μm.

Advanced Light Source (ALS) in Berkeley, CA. The microscope is jointly operated by the Center for X-ray Optics at the ALS, and the X-ray optical setup of XM-1 is described elsewhere.[13] Recent achievements in using Fresnel zone plates (FZP) for X-ray optics allow a spatial resolution down to 15 nm.[14,15] Synchrotron radiation emitted from a bending magnet is passed through the first FZP, a condenser zone plate, which provides both a partially coherent hollow-cone illumination of the specimen, and, in combination with a pinhole, serves as linear monochromator to select the proper wavelength. After transmission through the sample, a micro zone plate (MZP) projects a full-field image onto an X-ray sensitive CCD camera. For this study, a 35 nm MZP was used and imaged at a magnification of about 2000×. The illumination time per image was between 1 and 14 s. Each image covers a field of view of about 10 μm.

The liquid medium, composed of a saturated solution of calcium hydroxide (CH) and calcium sulfate dihydrate (gypsum, $C\bar{S}H_2$), was selected to provide sulfate ions to stimulate the formation of ettringite, and to simulate the chemical composition of the pore solution in fresh cement pastes. After mixing with an excess of solid gypsum and calcium hydroxide for 24 h, the solution was filtered twice. To avoid carbonation, the solution was prepared and stored in a glovebag filled with nitrogen gas. Also, to avoid the possibility of any reaction with laboratory glassware, polyethylene and Teflon beakers, flasks, and pipettes were used. Dispersions of both C_3A forms were prepared with the saturated solution, at solution/aluminate ratios of 5 mL/g, 10 mL/g, and 50 mL/g, corresponding to 0.4 g, 0.2 g, and 0.04 g of C_3A per 2 mL of the saturated solution, respectively. The solid particles were hand-mixed for 50 s into the solution and then centrifuged for 15 s. All samples were analyzed three times; the selected images presented in this paper summarize the behavior shown in all samples. In this study the solution/aluminate ratio is denoted as the initial solution/aluminate ratio ($s/a_{initial}$). During this first minute of hydration, it is expected that aluminum and calcium-bearing ions are released into the solution from the dissolution of the C_3A particles. The number of crystal nuclei formed during the initial period will be affected by the solution/aluminate ratio; the number of nuclei formed initially may then play an important role in determining the later growth rates of ettringite or other hydrates. To allow sufficient transmission of the soft X-rays, a small droplet (containing suspended small solid particles and nuclei) was taken from the supernatant solution and assembled in a specialized sample holder, comprising two silicon nitride windows, where the solution is squeezed in between the windows to an appropriate thickness and then imaged. This procedure is described in detail by Silva and Monteiro[16] and Monteiro et al.[17]

2.2.2. NMR Experimental Details. For NMR analysis, the same sample proportions were prepared, using C_3A powders as described above, and a saturated solution of gypsum and calcium hydroxide in fresh high purity deionized water which had been boiled for 30 min to minimize carbon dioxide content. Teflon and polyethylene flasks were again used. The suspensions were hand-mixed for 50 s and then centrifuged in a smaller plastic vial for 50 s in a centrifuge at 12,000 g. A 500 μL portion of the supernatant solution was transferred to a 5 mm NMR tube. All NMR spectra were acquired on a Bruker 600 AVANAC III spectrometer equipped with a Bruker BBO multinuclear probe at NMR core lab (King Abdullah University of Science and Technology, Kingdom of Saudi Arabia). The ^{27}Al NMR spectra were recorded by collecting 64 and 128 scans with a recycle delay time of 3s. Each spectrum was induced using a nonselective, 90-degree excitation pulse and digitized into 8 K complex data points. Spectra were recorded at ambient temperature (298 ± 1 K), and unlocked since the field drift was

(13) Meyer-Ilse, W.; et al. X-ray microscopy in Berkeley. In *X-ray Microscopy and Spectromicroscopy*; Thieme, J., et al., Eds.; Springer: Berlin, 1998; p I-1.
(14) Chao, W. *Nature* **2005**, *435*, 1210–1213.
(15) Kim, D.-H.; Fischer, P.; Chao, W.; Anderson, E.; Im, M.-Y.; Shin, S.-C.; Choe, S.-B. *J. Appl. Phys.* **2006**, *99*, 08H303.
(16) Silva, D. A.; Monteiro, P. J. M. *J. Am. Ceram. Soc.* **2007**, *90*, 614–617.
(17) Monteiro, P. J. M.; Kirchheim, A. P.; Chae, S.; Fischer, P.; MacDowell, A. A.; Schaible, E.; Wenk, H. R. *Cem. Concr. Compos. 31* (**2009**) 577−584

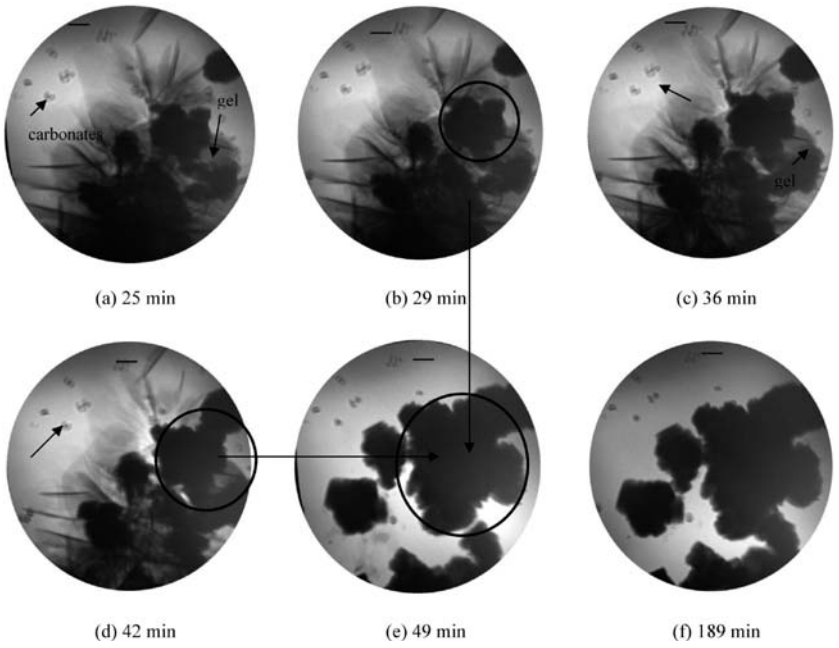

Figure 2. In situ soft X-ray images of hydrating orthorhombic C_3A particles in a saturated calcium hydroxide-gypsum solution, $s/a_{initial}$ = 5 mL/g. Hydration time is indicated. Scale bar corresponds to 1 μm.

negligible. Bruker Topspin 2.1 software was used in all experiments to collect and analyze the data, and all spectra were corrected by subtraction of the background contributions due to the probe head and tube.

3. Results and Discussion

3.1. Initial Solution/Aluminate Ratio = 5 mL/g. • **Cubic C_3A.** Figure 1 shows images of the process of cubic C_3A hydration in a saturated solution of calcium hydroxide and gypsum at a liquid/solid ratio of 5 mL/g; the images of the sample were taken in the same specimen at two different positions (Position 1 and Position 2). The images from Position 1, recorded from hydration times of 18 to 101 min, show the cubic C_3A particle (indicated by arrows) becoming covered by hydration products with needle-like morphology. The images of hydration evolution at Position 2, recorded from 50 to 88 min, show an agglomeration of ettringite needles, also indicated by arrows. Within a few minutes, all of the C_3A particles appear to be effectively completely hydrated, and the hydration products appear to nucleate and grow from sites inside the original particle boundaries to form clusters of needles, as shown in Figure 1. Three replicates of this mix were also analyzed, and each presented the same morphology. The density of cubic C_3A is 3030 kg/m^3, compared to values of 1768−1863 kg/m^3 for ettringite depending on its water content,[18] meaning that the complete hydration of C_3A necessarily requires expansion of the particle beyond its original boundaries. However, the nucleation site of each crystal does appear to be within the original particle boundaries.

In all images, the products of hydration are fibrous. The morphology identified suggests that crystals are acicular ettringite, which precipitates instantly upon hydration of the C_3A particles. Silva and Monteiro,[16] however, observed that cubic C_3A particles in the same type of solution resulted in C_3A particles being covered by a hydrated layer, which can be either continuous or discontinuous. However, X-ray diffraction and thermal analysis data presented by those authors revealed that their sample still contained 31% $Ca(OH)_2$, which was originally used as a raw material in synthesis of their C_3A. This is not present in the C_3A used here. The authors of that work justified their conclusion based on the arguments of Mehta,[19] who proposed that under high Ca^{2+} and OH^- concentrations, the microcrystalline hydrates tend to precipitate mostly on the surface of the C_3A particles because of the low extent of migration of $Al(OH)^-_4$ ions into the solution. These ions are instead arrested in the highly Ca^{2+} concentrated solution in the vicinity of the dissolving particle, forming hydrate products on the particle surfaces.

• **Orthorhombic C_3A.** Figure 2 shows large long fiber-like crystals, visible as needles, as well as hexagonal platelets that can be seen in a plan view (note the appearance of transparent hexagons) or a lateral view (note the long needles), with lengths of 3 to 5 μm, in a region with several particles of orthorhombic C_3A. The particles seem to be surrounded by a gel (indicated by arrows). These particles in the form of needles and platelets disappear over time; after 49 min they are no longer visible in the sample. There is then remarkably little change from 49 to 189 min. Note also that the orthorhombic C_3A particles show substantial swelling during hydration (as indicated by the changing circumference of the circle outlining a particular cluster of particles, from Figure 2(b) to images (d) and (e)), as the C_3A is apparently converted to ettringite by reaction in place. This differs from the behavior of the cubic C_3A sample at comparable liquid/solid ratio (Figure 1), where the ettringite crystals are much more needle-like and grow from the location of the original C_3A particle without retaining its morphology

(18) Balonis, M.; Glasser, F. P. *Cem. Concr. Res.* **2009**, *38*(9), 733–739.

(19) Mehta, P. K. *Cem. Concr. Res.* **1973**, *3*(1), 1–6.

so closely. Agglomeration of the hydrating particles is also observed during the reaction process.

In the orthorhombic specimen, the reactions evolved as expected until at 50 min of hydration; no further modifications were observed after this period. The morphology of the products of orthorhombic C_3A hydration in the same suspension ($s/a_{initial}$ = 5 mL/g) is completely different when compared to the cubic C_3A hydration in Figure 1. This does not in itself necessarily mean that the cubic phase is more reactive; however, it does mean that the hydration reaction proceeds in a different way, as is evident from the morphologies of the particles and products formed. These differences can be explained based on the ideas of Glasser and Marinho,[20] who proposed that the hydration of Na-doped C_3A (orthorhombic C_3A) can be summarized as occurring via the breakage of the Na−O bonds which leads to preferential release of alkali and the formation of mobile Na^+ ions. This leaves an Al-rich surface zone where Ca^{2+} is only partially hydrolyzed, and then a deeper zone which is depleted in Na but still contains most of its original Ca and Al.[11,20] In the vicinity of the alumina-rich zone, more general hydrolysis occurs, and the oxide sites which were formerly linked to Ca^{2+} and Al^{3+} convert to OH^- groups. These, together with appropriate cations, are available to participate in the formation of a reconstituted surface film. Ions steadily flow into the solution, whose ionic strength and basicity increases at least up to the point at which precipitations begin.

It should also be noted that the presence of Na in the reaction mixture is not expected to be sufficient to lead to the observed changes in morphology; Na addition to ettringite-forming mixtures has previously been observed to maintain the formation of the needle-like crystals formed in its absence.[21,22] The effects must therefore be mechanistic, and related to the differences in availability of the necessary nutrients required for ettringite growth from the two different precursors, as discussed above.

To confirm the observations with regard to solution chemistry and the higher concentrations of dissolved Al predicted in the orthorhombic C_3A samples, ^{27}Al solution NMR spectra were obtained from the supernatant phases of samples synthesized under the same experimental conditions as were used in the X-ray studies. Comparison of the ^{27}Al NMR spectra of the solutions present in equilibrium with the hydration products of orthorhombic and cubic C_3A confirms that there is a substantial difference in the dissolved Al concentrations present at equilibrium in the two systems, as shown in Figure 3. No octahedral sites were observed, which is consistent with the expected tetrahedral geometry of dissolved Al species at elevated pH; it is clear that the change to octahedral Al geometry in hydrate phases including ettringite occurs during crystallization rather than in the solution phase. The difference between the two samples in Figure 3 is a much more marked change than could be induced by the differences in solubility equilibria upon addition of a small amount of NaOH (equivalent to the effective

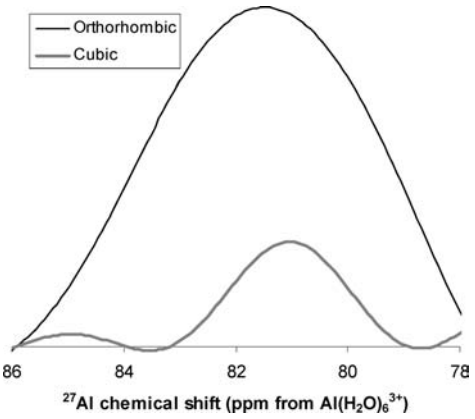

Figure 3. Tetrahedral Al regions of ^{27}Al NMR spectra of supernatant solutions from orthorhombic and cubic C_3A samples, $s/a_{initial}$ = 5 mL/g.

change in the solution chemistry because of the presence of Na in the orthorhombic C_3A). Damidot and Glasser[23] did observe a change in the dissolved Al concentration at the ettringite-gypsum-$Ca(OH)_2$-solution coexistence point in the $CaO-Al_2O_3-CaSO_4-H_2O$ system upon addition of Na_2O; however, this effect was approximately a doubling in Al concentration upon moving from zero to 0.05 M Na^+ concentration, and there was no further change upon increasing [Na^+] to 0.25 M. This contrasts with the results presented here, where there is more than a factor of 10 difference in the dissolved Al concentration between the two samples in Figure 3, with a total Na concentration (assuming all the Na initially present in the orthorhombic C_3A has become dissolved) of around 0.5 M.

3.2. Initial Solution/Aluminate Ratio = 10 mL/g. To evaluate the effect of higher sulfate ion concentrations in solution, and to facilitate the observation of the hydration process of cubic C_3A particles, the initial solution/aluminate ratio was increased to 10 mL/g.

• **Cubic C_3A.** At a higher solution/aluminate ratio (Figure 4), unlike the images shown in Figure 1, it is possible to observe the particles being hydrated over time, with the reaction visible more clearly and taking place more slowly.

From the beginning of the observable reaction period (Figure 4a), the particles are immediately covered by needle-like hydrates that grow in length and thickness over time (and most visibly between 53 and 79 min).

• **Orthorhombic C_3A.** Figure 5 presents images obtained at two different positions in the same sample of orthorhombic C_3A particles hydrating in a saturated calcium hydroxide-gypsum solution. Position 1 shows images from 40 to 120 min of hydration. Compared to cubic C_3A hydration, the presence of orthorhombic C_3A seemed to decrease the aspect ratio of ettringite crystals, while producing larger crystals. The same gel that appeared in Figure 4 can be seen again, and again is identified as a possible precursor of ettringite formation (Figure 5, Position 2). Some researchers[4,25] believe that there is a change in the morphology of the ettringite at the

(20) Glasser, F. P.; Marinho, M. B. *Br. Ceram. Soc. J.* **1984**, 35.
(21) Ogawa, K.; Roy, D. M. *Cem. Concr. Res.* **1982**, *12*(2), 247–256.
(22) Cody, A. M.; Lee, H.; Cody, R. D.; Spry, P. G. *Cem. Concr. Res.* **2004**, *34*(5), 869–881.
(23) Damidot, D.; Glasser, F. P. *Cem. Concr. Res.* **1993**, *23*(1), 221–238.
(24) Minard, H.; et al. *Cem. Concr. Res.* **2007**, *37*(10), 1418–1426.
(25) Billingham, J.; Coveney, P. V. *J. Chem. Soc., Faraday Trans.* **1993**, *89*(16), 3021–3028.

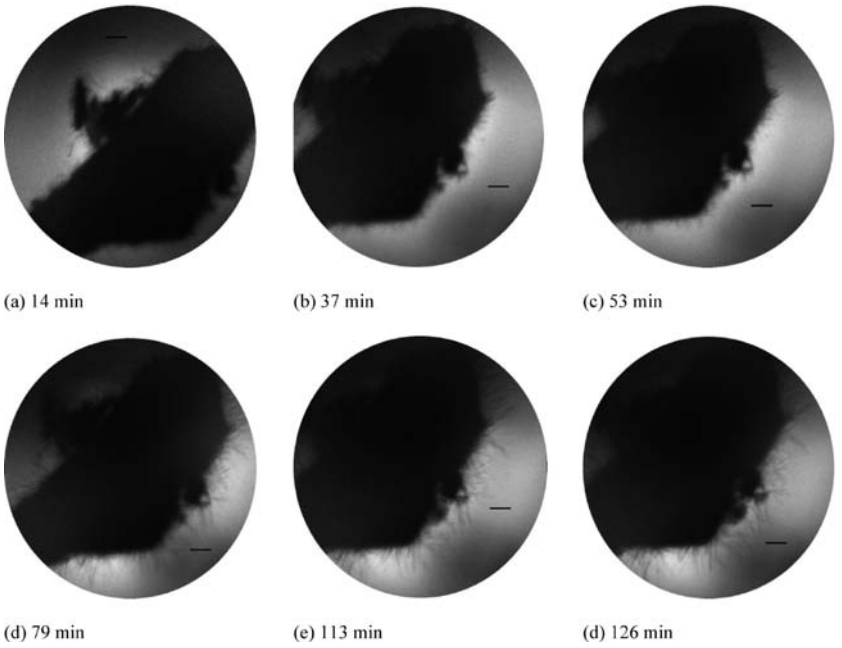

Figure 4. In situ soft X-ray images of hydrating cubic C_3A particles in a saturated calcium hydroxide-gypsum solution, $s/a_{initial} = 5$ mL/g. Hydration time is indicated. Scale bar corresponds to 1 μm.

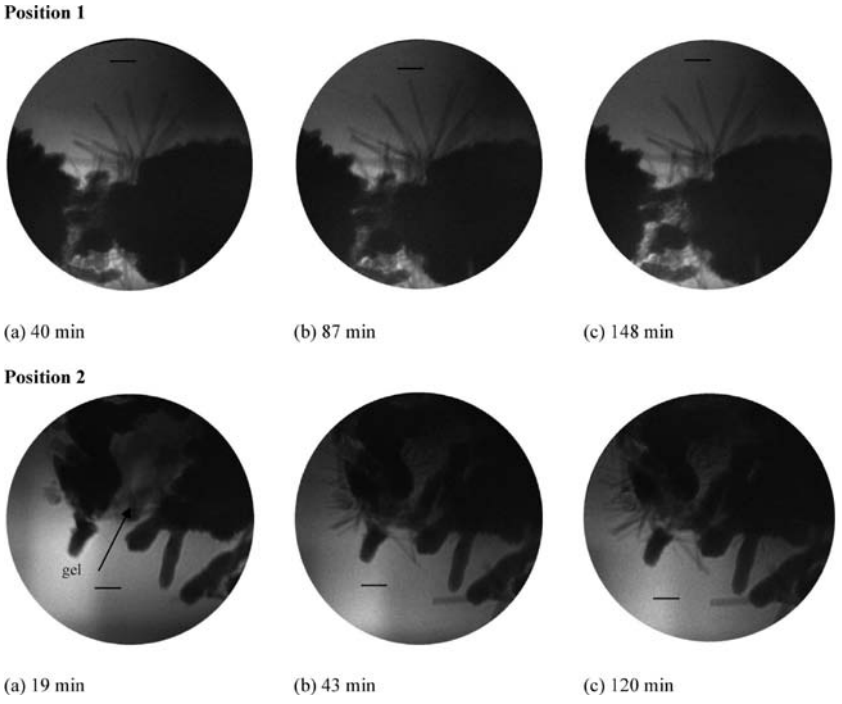

Figure 5. In situ soft X-ray images of hydrating orthorhombic C_3A particles in a saturated calcium hydroxide-gypsum solution, $s/a_{initial} = 10$ mL/g. Hydration time is indicated. Scale bar corresponds to 1 μm.

end of the induction period. This is initially deposited as a gel-like material and, according to this view, changes into a crystalline needle-like form. Unlike the assemblages of needle-like crystals, ettringite gel is believed to be impermeable to water. In a mixture containing cement and water, Billingham and Coveney[25] proposed that an initial jump in the slurry consistency in the early stages of hydration is due to the rapid formation of ettringite gel on mixing. Understanding this phenomenon is critical in controlling the workability of fresh Portland cement concrete, and the differences between the rates and products of orthorhombic and cubic C_3A hydration are therefore of potential importance in clinker design.

Both forms of C_3A when present at a concentration of $s/a_{initial} = 10$ mL/g presented differences in morphology when compared to the higher concentration analyzed above ($s/a_{initial} = 5$ mL/g); this can be attributed to the increased availability of sulfates to the hydrating particles, which allows ettringite formation closer to the C_3A particles. In summary: (a) the hydration of cubic C_3A

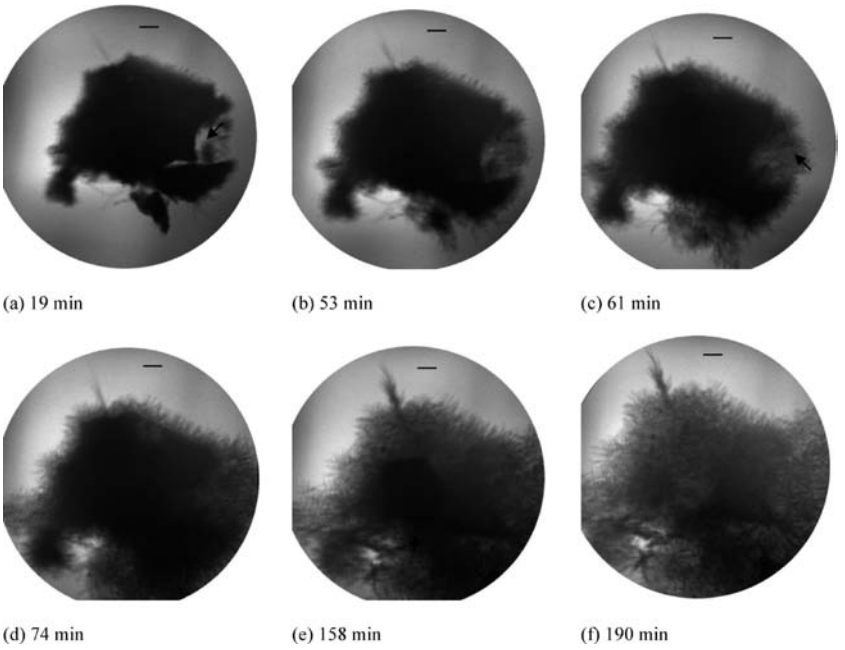

Figure 6. In situ soft X-ray images of hydrating cubic C_3A particles in a saturated calcium hydroxide-gypsum solution, $s/a_{initial} = 50$ mL/g. Hydration time is indicated. Scale bar corresponds to 1 μm.

results in ettringite needles forming along the surfaces of the particles, which are smaller than those observed in orthorhombic C_3A; and (b) in orthorhombic C_3A hydration an intermediate gel stage occurs before the formation of long ettringite needles.

3.3. Initial Solution/Aluminate Ratio = 50 mL/g. To complement the analysis of the effect of sulfate ion concentration and further verify the influence of the initial solution/aluminate ratio in the hydration reactions of cubic and orthorhombic C_3A, the liquid/solid ratio was increased to $s/a_{initial} = 50$ mL/g.

• **Cubic C_3A.** A sequence of images of the cubic C_3A particles hydrating under higher initial solution/aluminate ratio conditions is presented in Figure 6. These images are markedly different when compared to the previous images obtained at lower liquid/solid ratios. Here, it is possible to directly observe the needles growing, and eventually the complete dissolution of the C_3A particles occurs, with the original particles replaced via precipitation of clusters of very fine needle-like crystals of ettringite.

Figure 6 shows the hydration of the particles starting at around 11 min, with the C_3A particles first covered by small, fine hydrate hydrates, and then a rapid growth in both crystal length and thickness up to 53 min after mixing. After this period, the C_3A particle (which is by now completely covered by numerous needle-like hydrates) starts to swell as it becomes transformed to ettringite. From these images, the through-solution mechanism of ettringite formation can be seen; there is interfacial dislocation of outer products to inner products. The cubic C_3A particle, which initially showed a dense structure, is fully transformed into a much more open structure of ettringite needles after 190 min. The C_3A particle is completely consumed. The C_3A particle expands greatly from its original boundaries, and the observable space is mainly occupied by ettringite needles.

• **Orthorhombic C_3A.** Figure 7 presents images of orthorhombic C_3A particles hydrated for 54 min to 4 h in a saturated calcium hydroxide-gypsum solution. Note that the orthorhombic sample exhibits almost identical behavior to that observed for the cubic sample in Figure 6. A layer of small needles is readily visible growing on the surface of the particle, along with some swelling of the particle, as indicated by the arrows in images (a) and (c). One key difference between the cubic sample (Figure 6) and the orthorhombic sample (Figures 7 and 8) is the appearance of several long needles that form close and around the orthorhombic particle and in solution. Needles can also be observed far away from the particle in Figures 7 and 8, whereas all needles are closely associated with C_3A particles in Figure 6 for the cubic sample.

Figure 8 presents images taken from a different position in the same sample as Figure 7, with a smaller particle selected for analysis here. Figure 8 parts a−c also suggest that some of the initial products formed away from the surface of the C_3A may be lost, rather than formed, over time. This may be related to processes which could be described in terms of an Ostwald ripening mechanism, with the larger and more stable crystals growing at the expense of the small, high-surface area crystals. The growth of acicular hydrates occurs with greater intensity after 1 h; the reactions apparently stabilize after 2 h. Evidence for a through-solution mechanism (dissolution/precipitation) of ettringite formation can also be seen in Figure 8, with the crystals obviously growing at the ends further from the C_3A particle by deposition of dissolved species. A comparison between the orthorhombic particles shown in Figure 8 with the cubic particles shown in Figure 6 shows that the orthorhombic C_3A leads to the formation of larger and thicker needle-like crystals over time. Comparing Figures 7 and 8, the variation in behavior between smaller and larger grains is obvious.

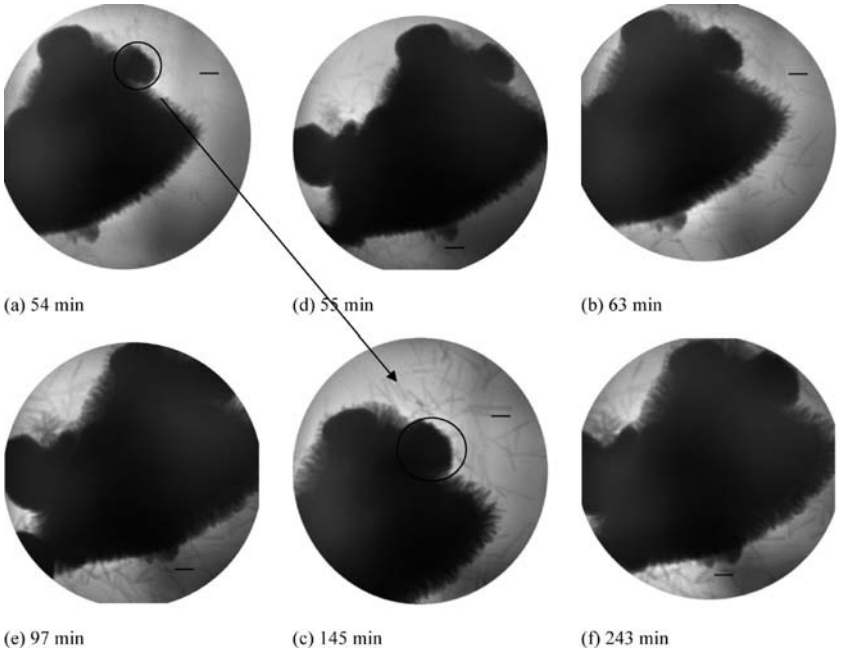

Figure 7. In situ soft X-ray images of hydrating orthorhombic C_3A particles in a saturated calcium hydroxide-gypsum solution, $s/a_{initial}$ = 50 mL/g. Hydration time is indicated. Scale bar corresponds to 1 μm.

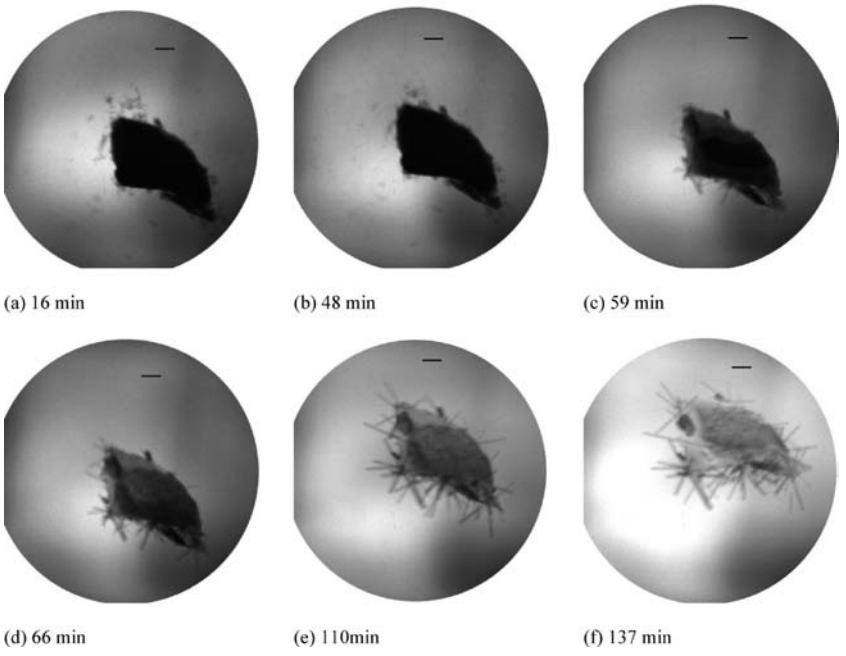

Figure 8. In situ soft X-ray images of hydrating orthorhombic C_3A particles (a smaller original particle than shown in Figure 7), in a saturated calcium hydroxide-gypsum solution, $s/a_{initial}$ = 50 mL/g. Hydration time is indicated. Scale bar corresponds to 1 μm.

Contrary to the results obtained in more concentrated reaction systems ($s/a_{initial}$ = 5 and 10 mL/g), in this suspension ($s/a_{initial}$ = 50 mL/g) the through-solution mechanism of ettringite formation can be observed for both specimens (cubic and orthorhombic). The through-solution mechanism can be distinguished from ion exchange and absorption processes by observation of the product morphologies. To provide further confirmation of this result, ^{27}Al NMR spectra were obtained for the supernatant solutions of the more dilute samples, as well as for samples taken from the $s/a_{initial}$ = 5 mL/g sample as a function of reaction time. However, the concentrations of dissolved Al in the 10 and 50 mL/g samples were too low to be observed by ^{27}Al NMR, and the Al concentration and coordination state in the 5 mL/g samples remained remarkably constant as a function of reaction time before extraction of the supernatant (from 5 min to 1 h).

Finally, it is interesting to note that in all images collected for both the cubic and the orthorhombic samples reacting under the conditions studied here, the reactions are essentially complete after 50 min of hydration,

which is not the case for C_3A in a reacting Portland cement system. This is explained by the higher interparticle distance (because of the need to study dilute systems in X-ray microscopy) and the higher sulfate ion concentration in these systems when compared to the amount of gypsum interground with Portland cement. In a cement matrix, a high water/cement ratio has been shown to lead to a higher rate of diffusion of the ions in the pore solution, which leads to the formation of more ettringite crystals, especially away from the surface of cement particles,[9] but also has detrimental effects on the strength and durability of the hardened cement product.

Any crystallization process comprises three basic steps: achievement of supersaturation, formation of crystal nuclei, and growth of particles.[26] A difference in chemical potential between solid and aqueous phases becomes the driving force for dissolution (in the case of undersaturation) or precipitation (in the case of supersaturation). Once nuclei form in a supersaturated solution, they begin to grow by accretion and, as a result, the concentration of the remaining dissolved species drops. Thus, there is a competition for material between the processes of nucleation and crystal growth. The more rapid the nucleation, the larger the number of nuclei formed before the dissolved species concentrations drop below supersaturation, resulting in smaller final crystals. Brown and LaCroix[27] determined that the nucleation process in ettringite formation from solution was diffusion controlled. It has also been suggested that the C_3A surface may serve as a vehicle for ettringite nucleation,[28] and Silva and Monteiro[16] did observe ettringite growth on or near the surface of cubic C_3A particles. On the other hand, Minard et al.[24] assumed that while the slow process of ettringite formation could be limited by ettringite growth rate, its dependence on the surface area of C_3A indicated that it is limited by dissolution of C_3A.

Minard et al.[24] also described their observations that, even with different C_3A reactivities, the time necessary to exhaust the sulfate ions in solution does not relate in a linear way to the quantity of gypsum initially introduced. In the present research, the hydration of (pure) cubic C_3A seems to be more susceptible to the presence of a higher concentration of sulfate ions, considering that there are less C_3A particles in solution for the same initial sulfate concentration. The crystal growth of the hydration products from the cubic C_3A involved a larger number of nuclei, which led to a smaller crystal size, depending on the concentration of sulfate ions. The higher the sulfate/C_3A ratio, the smaller the size of ettringite needles, and the faster the consumption of the entire particle of C_3A. All orthorhombic C_3A (Na-doped) samples were characterized by the growth of larger ettringite needles, with the appearance of an intermediate gel stage before the formation of long ettringite needles. For the orthorhombic samples, the higher the sulfate concentration, the smaller are the ettringite crystals, with a longer time required to exhaust the C_3A. Corroborating these observations, but using different mixture proportions to synthesize solid samples rather than the slurries studied here, Kirchheim et al.[11] showed using SEM that, based on the size of ettringite crystals formed and the extent of consumption of C_3A and gypsum, orthorhombic C_3A pastes presented a faster rate of formation of crystals. The ettringite crystals were also longer for the orthorhombic C_3A samples in that investigation, showing that the dilution of the systems for X-ray microscopy study here has maintained the key mechanisms and trends observed in more "realistic" lower-liquid systems. Real time rheometric measurements[11] showed that orthorhombic C_3A mixes presented a more rapid increase of stiffness than cubic C_3A mixes in the very early stages of hydration, which can again be attributed to the higher reactivity of the orthorhombic C_3A in the presence of sulfates.

5. Conclusion

The results of analysis of the hydration of cubic and orthorhombic C_3A in saturated lime and gypsum solutions can be summarized as follows:

- Na-doped orthorhombic C_3A reacts more rapidly than pure cubic C_3A in forming hydration products, which are predominantly ettringite
- The ettringite needles formed by hydration of orthorhombic C_3A are in many cases larger and with lower aspect ratio than those formed from cubic C_3A
- At a very high initial solution/aluminate ratio ($s/a_{initial}$ = 50 mL/g), the greater amount of sulfate available to react with each aluminate species released from the C_3A and higher extent of dilution allowed for observation of the complete dissolution of C_3A particles and precipitation of ettringite crystals by a through-solution mechanism
- For the $s/a_{initial}$ = 10 mL/g system, the formation of needles was observed near the surface of particles of cubic C_3A, and a gel appeared between the particles of orthorhombic C_3A, which was followed by the formation of ettringite needles from (and replacing) this gel
- For the $s/a_{initial}$ = 5 mL/g solution, the products of hydration formed almost instantaneously for systems involving both forms of C_3A The cubic C_3A grew, almost instantaneously, acicular crystals. For the orthorhombic C_3A samples, a gel and hexagonal platelets appeared close to the particles. All reactions had occurred before 50 min of hydration.

Soft X-ray microscopy has been shown to be an interesting in situ techique to study the real-time hydration of cement phases, particularly cubic and orthorhombic C_3A in this paper, providing valuable information about the morphology and growth rates of the hydration products, and their dependence on the details of the anhydrous precursor.

Acknowledgment. A.P.K. acknowledge the financial support of CAPES, CNPq of The Brazilian Ministry of Education, and FAPERGS (Rio Grande do Sul Foundation to Support Research) and is grateful to Dong-Hyun Kim and Anne Sakdinawat (Center for X-ray Optics) for their assistance in acquiring the X-ray images. This publication was based on work supported in part by Award

(26) Mullin, J. W. *Crystallization*; Butterworths: London, 1961.
(27) Brown, P. W.; LaCroix, P. *Cem. Concr. Res.* **1989**, *19*, 879–884.
(28) Pommersheim, J.; Chang, J. *Cem. Concr. Res.* **1988**, *18*(6), 911–922.

No. KUS-l1-004021, made by King Abdullah University of Science and Technology (KAUST). The operation of the microscope is supported by the Director, Office of Science, Office of Basic Energy Sciences, Materials Sciences and Engineering Division, of the U.S. Department of Energy under Contract No. DE-AC02-05-CH11231. The participation of John Provis in this work was supported by the Banksia Foundation, Australia, through the awarding of the Brian Robinson Fellowship, as well as by the Australian Research Council.